Detecting landslide-induced paleolakes and their impact on river courses

Anne-Laure Argentin(1), Günther Prasicek(1,2), Jörg Robl(1), Daniel Hölbling(3), and Barbara Friedl(3)

(1) University of Salzburg, Department of Geography and Geology, Hellbrunner Strasse 34, 5020 Salzburg, Austria
(2) University of Lausanne, Institute of Earth Surface Dynamics (IDYST), Quartier UNIL-Mouline, Bâtiment Géopolis, 1015 Lausanne, Switzerland
(3) University of Salzburg, Department of Geoinformatics — Z_GIS, Schillerstrasse 30, 5020 Salzburg, Austria

anne-lauremarine.argentin@sbg.ac.at

EGU2018-6349

ÖAW ÖSTERREICHISCHE AKADEMIE DER WISSENSCHAFTEN

This presentation participates in OSPP
EGU
Outstanding Student Poster & PICO Contest

Introduction

Landslides are one of the most destructive natural hazards in mountainous area. They endanger human lives and infrastructures by their direct consequences and by the river changes they infer. One of those changes is the damming of the local river. A lake forms upstream of the landslide deposits, flooding the area, and if the dam breaks, the water is released in a devastating flood. If not, the lake may fill entirely with sediments.

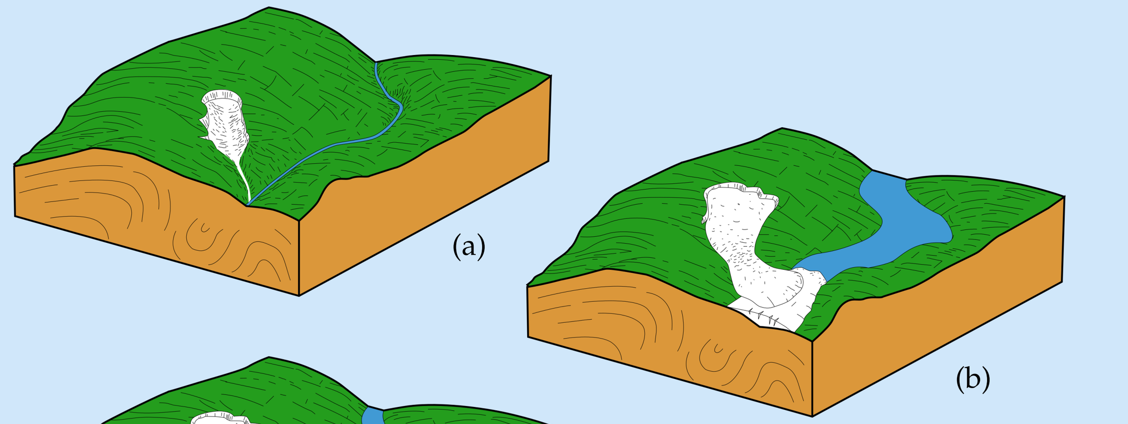

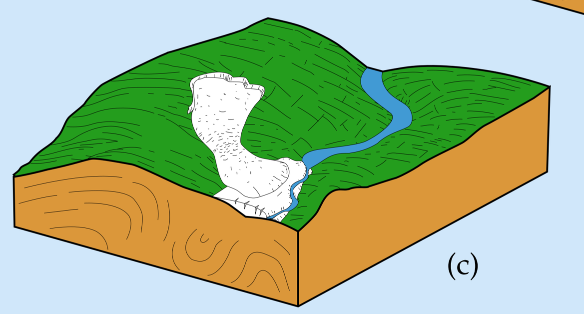

Fig. 1: Landslide of Creux-du-Van dams the Val-de-Travers. (a) Landslide begins. (b) Landslide dams the river, sedimentation. (c) Dam break or overtopping.

We wanted to assess the persistence of paleolake landforms in mountainous areas, so we created a wide and flat valley segment index (WFi).
Here we compare three different landslide-induced paleolakes: the Val-de-Travers paleolake, the Tsaoling paleolake and the Ilanz paleolake.

Methods

Inputs

- SRTM Digital Elevation Data Version 4, 3 arc-seconds
- WWF HydroSHEDS Drainage Direction, 3 arc-seconds
- Google Earth Engine Slope

Construction of river trees

Hydrological model:
river
subwatershed
interwatershed
interwatershed boundary

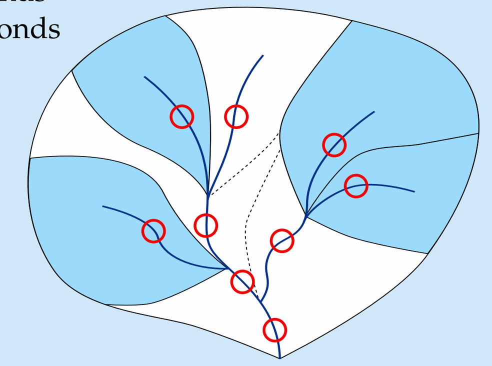

Fig. 1: Structure of a river network from Demir and Szczepanek, 2017, [1]. Each river branch (symbolized by a red circle) is stored separately.

Each drainage network is stored as a river tree (Fig. 1) [1]. It allows a comparison of the different branches in a way that takes into account the topology of the network.

Compute the slope rest index (SRi)

SRi = Current max slope - pixel slope

with the current max slope being recorded from downstream on (Fig. 2).

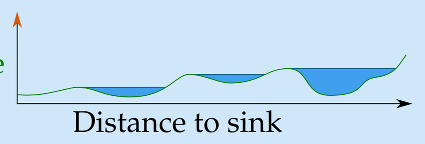

Fig. 2: The slope rest index is indicated by the blue surface. It is the difference between the local slope and the maximal upstream slope.

Compute the valley concavity index (VCi)

$$ax^2 + by^2 + cx + dy + e = 0$$

We fit a quadratic surface to the surrounding pixels (Fig. 3).

$$VCi = max(a, b)$$

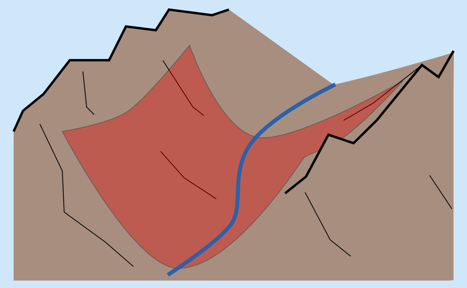

Fig. 3: The valley flanks are fitted with a quadratic surface (red) [2] to compute the valley concavity index.

Compute the flat and wide valley segment index (FWi)

$$FWi = SRi * VCi$$

Val-de-Travers paleolake and Creux-du-Van landslide, Jura, Switzerland

Acording to Matthey [3], the Creux-du-Van landslide (Fig. 4) happened due to bank erosion around 10.350 – 10.000 B.C.. The landslide dammed the river and formed the Val-de-Travers lake. The lake disapeared around 4.000 – 2.500 B.C. because it had entirely sedimented.

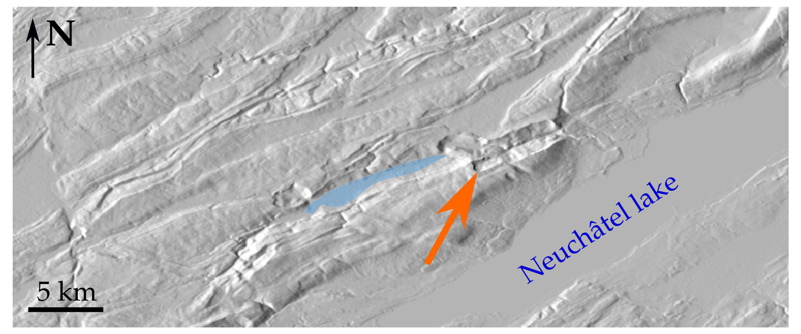

Fig. 4: The hillshade view of the Val-de-Travers study area. The Creux-du-Van (orange) originated a landslide that formed the Val-de-Travers paleolake (blue).

The flow accumulation is computed with the D8 algorithm based on the WWF HydroSHEDS Drainage Direction, 3 arc-seconds. The drainage network is extracted using a flow accumulation threshold of 500 pixels. We store the river network topology into memory using a river tree [1] onto which we compute and enter several attributes.

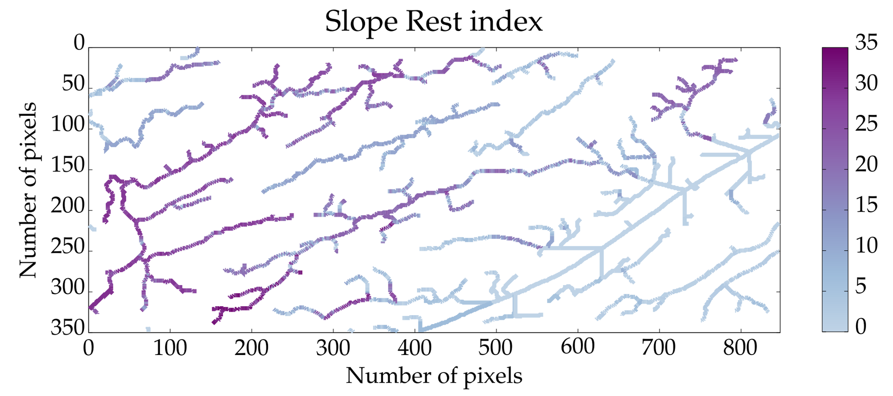

Fig. 5: We use the slope computed from the SRTM Digital Elevation Data Version 4, 3 arc-seconds, using the ee.Terrain algorithm from Google Earth Engine to compute the slope rest index.

The SRi (Fig. 5) highlights the knickpoints in the river network. Here, all the region upstream of the dam has a higher index.

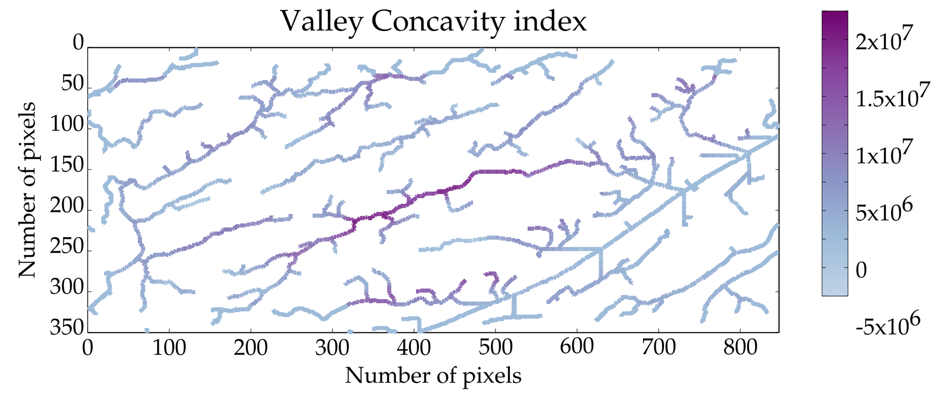

Fig. 6: The valley concavity index has been computed using a 33 x 33 pixels moving window.

The valley concavity index is computed on all pixels of the river network (Fig. 6). The Val-de-Travers has a high valley concavity index.

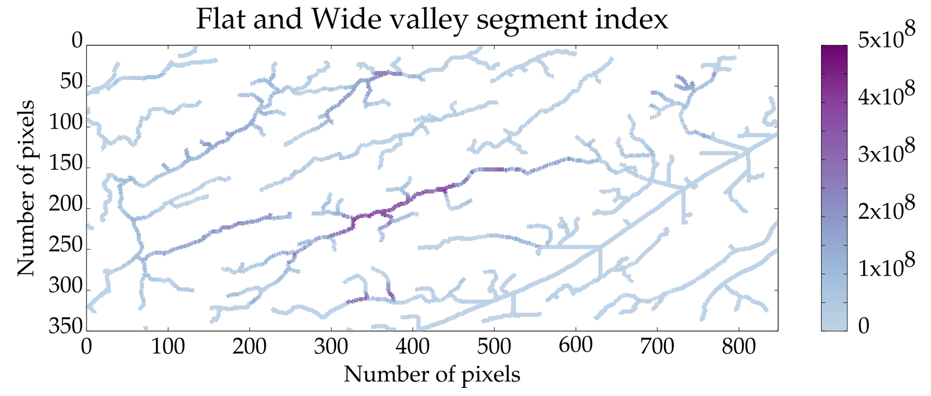

Fig. 7: The flat and wide valley segment index highlights the Val-de-Travers.

The FWi (Fig. 7) highlights the Val-de-Travers as the largest flat and wide valley segment of our study area. We know this landform is due to the landslide-induced paleolake.

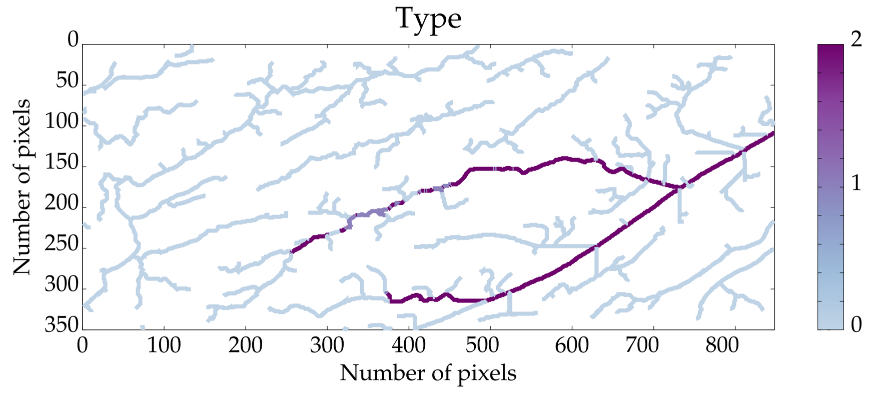

Fig. 8: The pixel type is the position of the pixel in relation to the paleolake; 0: no paleolake upstream, 1: paleolake pixel, 2: a paleolake is detected upstream of the pixel.

We classify the pixels according to their location in relation with the paleolake (Fig. 8).

Principal Component Analysis of the results

We correlate the results of the paleolake detection with other attributes such as sinusosity, normalized steepness index, Strahler order, to detect some possible consequences of the paleolake on the river network (Fig. 9).

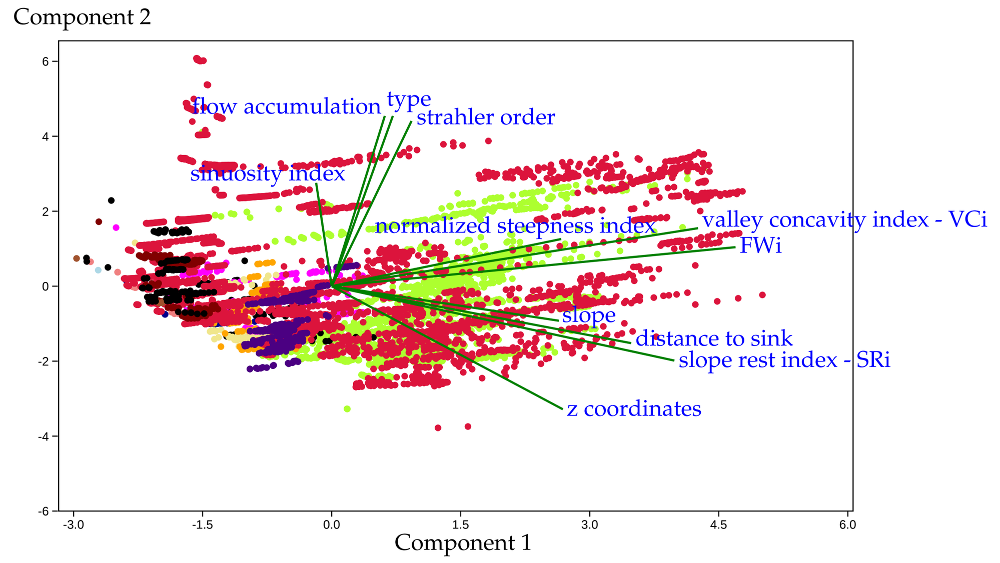

Fig. 9: Principal Component Analysis of all the data stored for the Val-de-Travers study area. Each river network has a different color. In red the river network affected by the paleolake.

According to the correlation circle, the type of pixel is highly correlated to the Strahler order and the flow accumulation, as well as the sinuosity index, in a lesser importance. They are all almost uncorrelated to the slope, the distance to sink and the slope rest index.

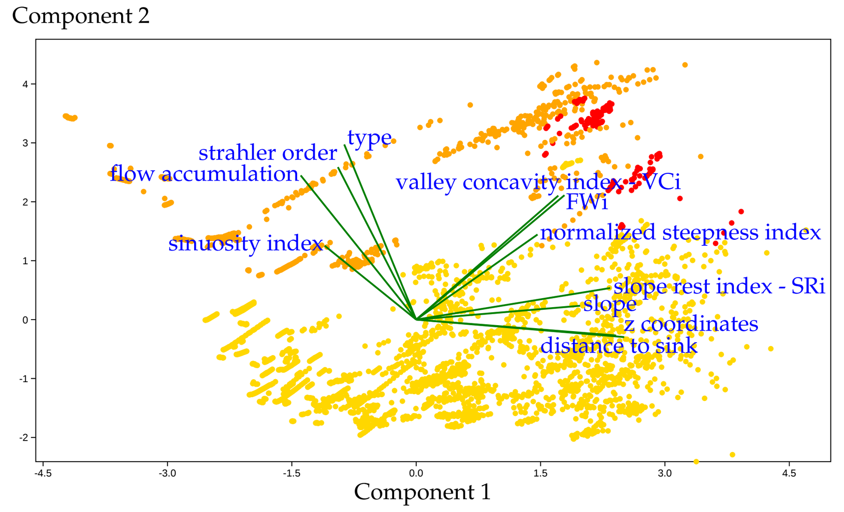

Fig. 10: Principal Component Analysis of the paleolake-affected river network. Each type of pixel is a different color. Red: paleolake pixel, Orange: affected pixel, Gold: unaffected pixel.

The results on the affected river network (Fig. 10) show approximately the same correlation circle as the analysis on the entire map. According to the correlation circle, the sinuosity is uncorrelated to the FWi, but is slightly correlated to the type.

Tsaoling rockslide, Taiwan

5 landslide-dam events took place from 1862 to 1999 in the Tsaoling region [4]. The event from 1999 was due to the 921 (a.k.a. Jiji) earthquake and formed a lake of 42,000,000m^3 on the Chingshui river (Fig. 11). Several typhoons contributed to the sedimentation of the lake until its filling in 2004.

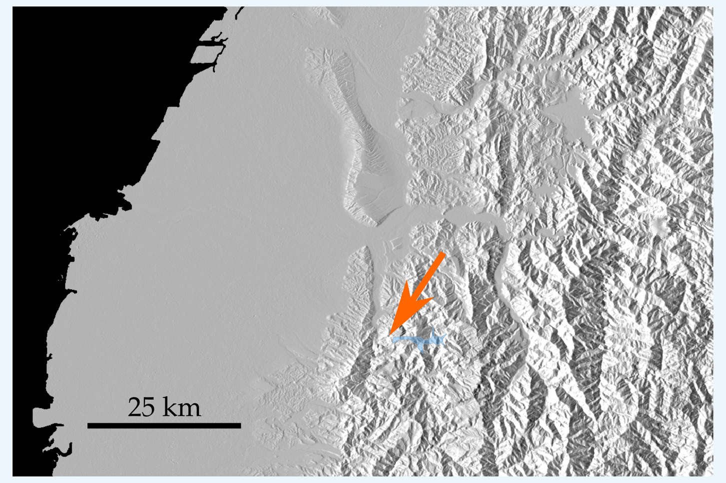

Fig. 11: The hillshade view of the Tsaoling study area. The Tsaoling landslide originated from the orange arrow and formed the lake (blue).

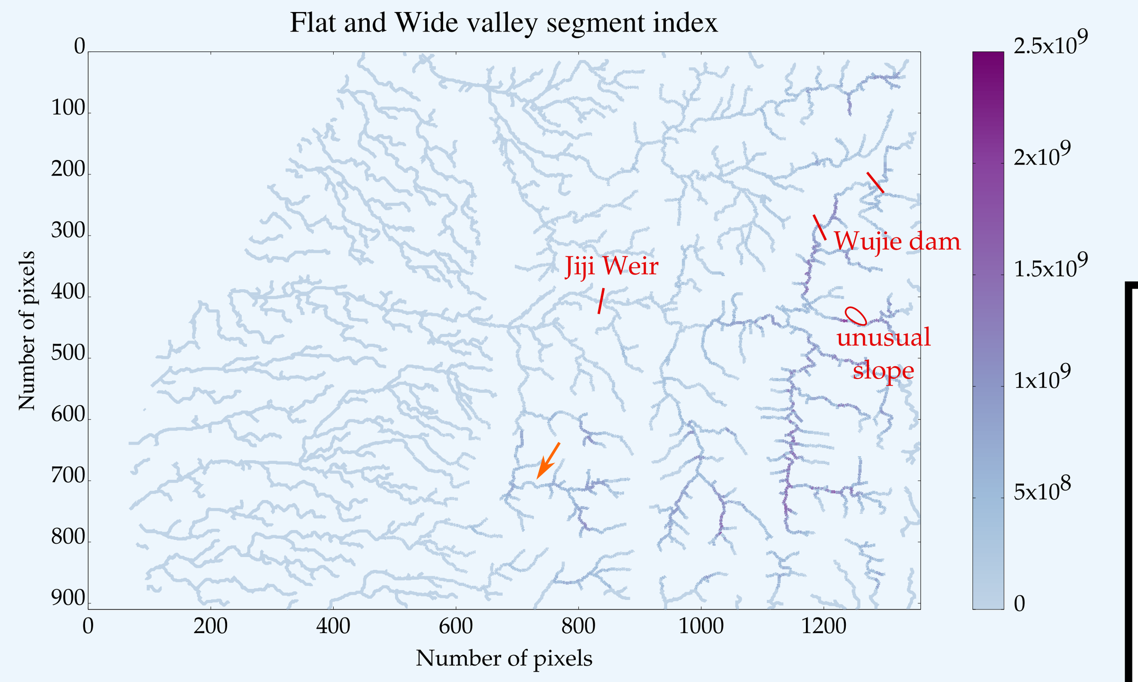

Fig. 12: The FWi does not highlight the lake (right of the orange arrow) as a flat and wide region, unlike the Eastern part of the river network.

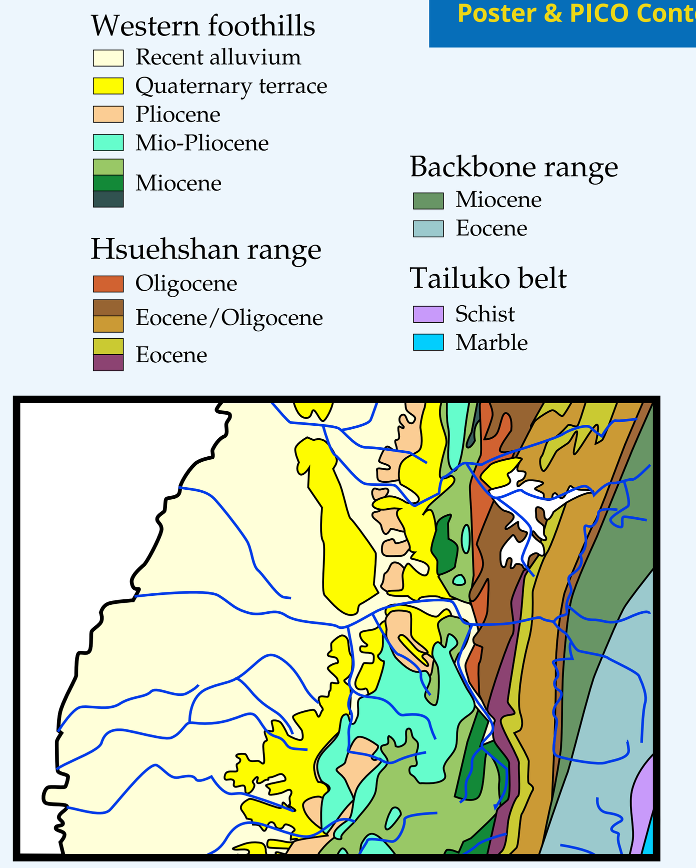

Fig. 13: The geological map of Taiwan, modified from Chen et al., 2000 [5].

The SRTM data was acquired 6 months after the Jiji earthquake, and the water level had not yet risen to a high enough level to have a good valley concavity index, and FWi. The catchments situated on the Hsuehshan Range, parallel to the Lishan major thrust, have higher FWi (Fig. 12). Those results can be explained by the geological features of Taiwan (Fig. 13). This may be related to variations in bed-rock erodability or uplift rate, anthropogenic impact or increased sediment supply from the hillslopes.

Ilanz paleolake and Flims rockslide, Alps, Switzerland

The Flims rockslide was triggered in 8200 – 8300 yrBP [6]. It dammed the Rhein river and formed the Ilanz paleolake, of estimated volume of about 1,5km^3 (Fig. 14). It is assumed that the dam broke in a catastrophic event, approximately 1000 years after its creation.

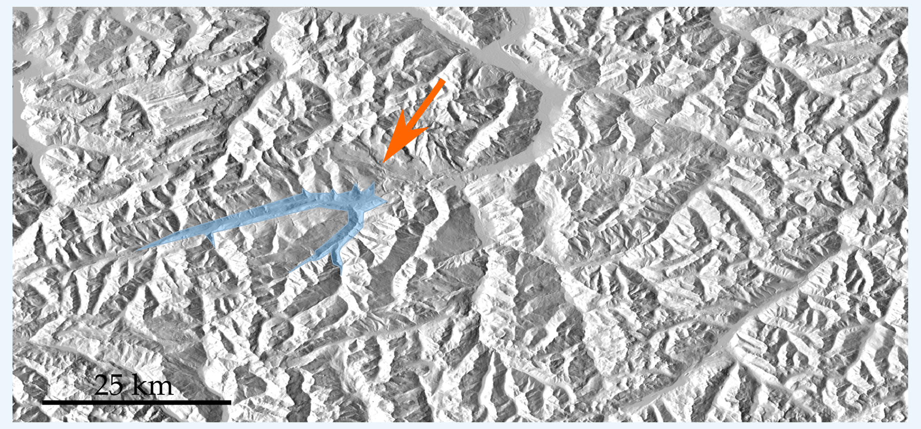

Fig. 14: The hillshade view of the Ilanz study area. The Flims rockslide originated from the orange arrow and dammed the Rhein river, forming the Ilanz paleolake (blue).

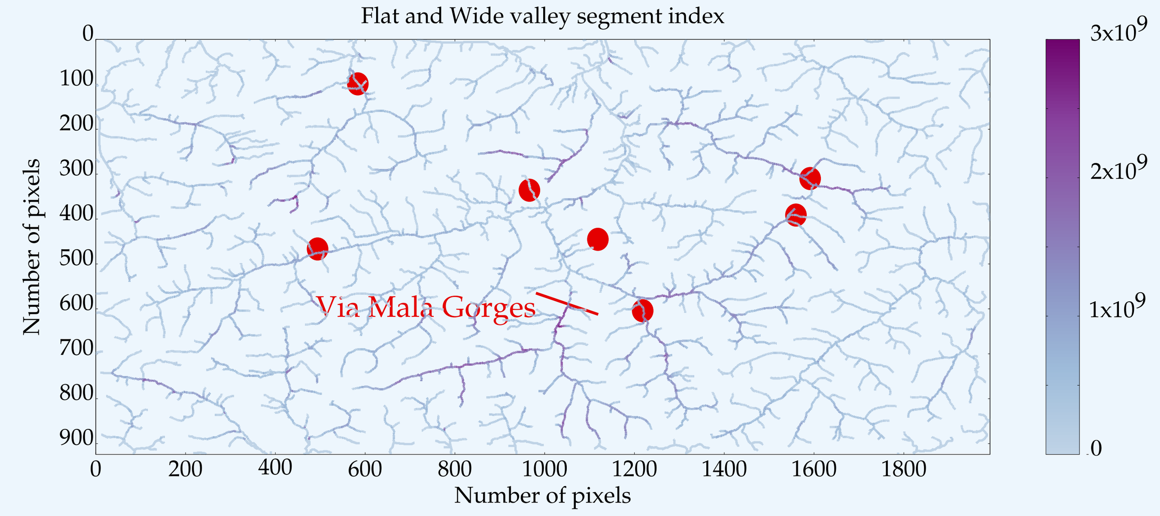

Fig. 15: The FWi highlights the eastern branches of the river network. The red dots indicate the major landslides in the area.

The Ilanz paleolake does not present a high FWi (Fig. 15) because the Flims landslide deposits were already swept away of the river bed. This may be due to the water being released during a catastrophic dam break which was very efficient in eroding the sediments. The gorges of Via Mala, on the contrary, present a high slope change which explains the high FWi upstream of it.

Summary:

The detection of landslide-induced changes of the valley geometry represents a valuable approach to quantify the frequency of catastrophic landslides and related secondary effects (e.g. floodings after dam-breaks) on a regional scale. Therefore we have developped a series of novel numerical tools:

- A topology-based data storage method for the study of river networks.
- An associated comparison method of river caracteristics based on the location in relation to the paleolake (or any other event happening locally).
- An index to detect flat and wide/concave valley segments.

Conclusions:

We have successfully applied the FW index to detect paleolakes. However the interpretation of the FWi is not unique, as the index is also sensitive to geological peculiarities.

We carried out a PCA on the attributes of the river network. The sinuosity may be correlated to the type of pixel (paleolake, affected, unaffected), although analysis of other river networks impacted by paleolakes are needed to confirm this trend.

Future work will focus on:

Further work will imply:
- the addition of some other characterizing attributes to the river network.
- the application of the topology-based analysis to satellite imagery.
- the variations of the results depending on external factors like the type of paleolake break (catastrophic event, slow filling), the volume of the event (triggering landslide, resulting lake).
- a study on how to establish causal relationships (not only correlations) between events happening without the processes at stake being observed.

[1] Demir, I. and Szczepanek, R., 2017. Optimization of river network representation data models for web-based systems, Earth and Space Science, 4, 336–347, doi:10.1002/ 2016EA000224.
[2] Prasicek, G., et al., 2015. Tectonic control on the persistence of glacially sculpted topography. Nature communications, 6, 8028.
[3] Matthey, F., 1971. Contribution à l'étude de l'évolution tardi- et postglaciaire de la végétation dans le Jura central, Matériel pour le levé géobotanique de la Suisse, Hans Huber, Berne.
[4] Hsu, Y. and Hsu, Y., 2009. Impact of earthquake-induced dammed lakes on channel evolution and bed mobility: Case study of the Tsaoling landslide dammed lake. Journal of Hydrology, 374, 1-2, 43-55.
[5] Chen, C.-H., et al. 2000. Geological Map of Taiwan. 1:500,000 scale, Central Geological Survey, Taiwan.
[6] von Poschinger, A., 2011. The Flims rockslide dam. In Natural and Artificial Rockslide Dams. Springer, Berlin, Heidelberg, 407-421.

UNIVERSITÄT SALZBURG
geomorphology.sbg.ac.at